Autosomal Dominant Craniometaphyseal Dysplasia Is Caused by Mutations in the Transmembrane Protein ANK

Ernst Reichenberger,[1] Valdenize Tiziani,[1,4] Shoji Watanabe,[1,5] Lucy Park,[1] Yasuyoshi Ueki,[1] Carla Santanna,[1] Scott T. Baur,[1,2] Rita Shiang,[6] Dorothy K. Grange,[7] Peter Beighton,[8] Jessica Gardner,[8] Herman Hamersma,[8] Sean Sellars,[8] Rajkumar Ramesar,[8] Andrew C. Lidral,[9] Annmarie Sommer,[10] Cassio M. Raposo do Amaral,[4] Robert J. Gorlin,[11] John B. Mulliken,[3] and Bjorn R. Olsen[1]

[1]Harvard-Forsyth Department of Oral Biology, The Forsyth Institute, Harvard School of Dental Medicine, and Department of Cell Biology, [2]Department of Genetics, and [3]Division of Plastic Surgery, Children's Hospital, Harvard Medical School, Boston; [4]Universidade Federal de São Paulo–EPM and Instituto de Cirurgia Plástica Craniofacial SOBRAPAR, Campinas, Brazil; [5]Department of Plastic and Reconstructive Surgery, Showa University School of Medicine, Tokyo; [6]Department of Human Genetics, Medical College of Virginia, Richmond; [7]Division of Medical Genetics, Cardinal Glennon Children's Hospital, Saint Louis University School of Medicine, St. Louis; [8]Department of Human Genetics, University of Cape Town Medical School, Observatory, South Africa; [9]Department of Orthodontics, Ohio State University, College of Dentistry, and [10]Department of Genetics, Children's Hospital, Columbus; and [11]Department of Oral Biology and Genetics, University of Minnesota School of Dentistry, Minneapolis

Craniometaphyseal dysplasia (CMD) is a rare skeletal disorder characterized by progressive thickening and increased mineral density of craniofacial bones and abnormally developed metaphyses in long bones. Linkage studies mapped the locus for the autosomal dominant form of CMD to an ~5-cM interval on chromosome 5p, which is defined by recombinations between loci D5S810 and D5S1954. Mutational analysis of positional candidate genes was performed, and we describe herein three different mutations, in five different families and in isolated cases, in ANK, a multipass transmembrane protein involved in the transport of intracellular pyrophosphate into extracellular matrix. The mutations are two in-frame deletions and one in-frame insertion caused by a splicing defect. All mutations cluster within seven amino acids in one of the six possible cytosolic domains of ANK. These results suggest that the mutated protein has a dominant negative effect on the function of ANK, since reduced levels of pyrophosphate in bone matrix are known to increase mineralization.

Introduction

Autosomal dominant (AD) craniometaphyseal dysplasia (CMD [MIM 123000]) (Jackson et al. 1954) is a rare skeletal condition that involves abnormal bone formation and mineralization in membranous as well as endochondral bones. Increased density of craniofacial bones, beginning at the base of the skull, can be diagnosed during early childhood. Sclerosis is accompanied by progressive thickening of the bones, which can cause narrowing of cranial foramina and can lead to severe visual and neurological impairment, such as facial palsy and deafness. Typical facial features of CMD include a wide nasal bridge, paranasal bossing, and orbital hypertelorism (fig. 1). Metaphyses of long bones are widened (Erlenmeyer flask-shaped) and exhibit decreased

density (fig. 1). Diaphyses show normal patterns of trabeculation; however, the cortex can be thicker in some instances.

Thickened cranial bones or flared metaphyses are not unique to CMD and are seen in a number of skeletal disorders. Many of these conditions are very rare, and differential diagnosis can be difficult. CMD is clinically distinct from other craniotubular disorders such as craniodiaphyseal dysplasia (MIM 218300), Pyle disease (MIM 265900), osteopathia striata with cranial sclerosis (MIM 166500, frontometaphyseal dysplasia (MIM 305620), and sclerosteosis (MIM 269500). Sclerosteosis is the only disorder for which the causative gene (*SOST*) has been identified (Balemans et al. 2001; Brunkow et al. 2001).

CMD occurs in an AD and an autosomal recessive (AR) form (MIM 218400) (Gorlin et al. 1969). Sclerosis of cranial bones is usually much more severe in the rare AR form. AR CMD has recently been mapped to a 7-cM interval on chromosome 6q21-22 (Iughetti et al. 2000). A genetic locus for the AD form of CMD, encompassing 19 cM on chromosome 5p15.2-p14.1 (Nurnberg et al. 1997), has been reported for a large pedigree of German origin. An 11-cM interval in the
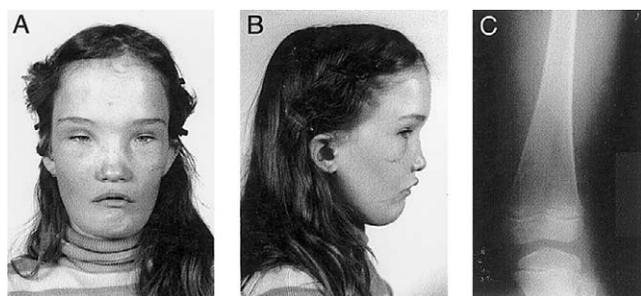
Figure 1   *A* and *B*, Proband of pedigree A, at age 12, showing typical features of CMD—for example, hypertelorism, wide nasal bridge, and paranasal bossing. *C*, Metaphyseal flaring in a 2-year-old child from family C.

same locus has been determined for a South African kindred (J. Gardner, P. Beighton, H. Hamersma, S. Sellars, and R. Ramesar, unpublished data).

We have independently mapped CMD to the 5p locus and have defined a 5-cM interval by means of linkage studies and haplotype analysis. Mutational analysis of candidate genes within this locus revealed sequence variants in the transmembrane protein ANK. Herein we show that mutations in ANK cause CMD in several sporadic cases and in families with AD inheritance of CMD.

Subjects and Methods

Subjects

Familial and sporadic cases of CMD were contributed by clinical collaborators (D.K.G., P.B., J.G., H.H., S.S., R.R., A.S., A.C.L., A.S., R.J.G., C.R.A., and J.B.M.) in accordance with the regulations of their institutional review boards and the Institutional Review Board of Harvard Medical School. Participating subjects were eval-

uated clinically, and peripheral blood samples were obtained.

Genomewide Screening and Physical Map

DNA isolation, genomewide screening, and linkage analysis were performed as described elsewhere (Tiziani et al. 1999). Information about additional markers and physical clones was obtained from the literature (Church et al. 1997), the Lawrence Berkeley National Laboratory Sequence Archive, the Genome Database, GenBank, and the Celera database. New microsatellite markers were developed by cycle sequencing of (CA)n microsatellites from the genomic clones directly, using degenerate (GT)8 primers (Hawkins et al. 1994). BAC and PAC clones were obtained from BACPAC Resources.

Mutation Analysis

Exons of candidate genes were amplified with primers in flanking intron sequences, using genomic DNA of affected individuals. Intronic sequences were available in either GenBank (accession numbers AC010491 and AC026437) or the Celera Discovery System (Celera Genomics; accession number GA_65585516). Primers used to amplify ANK exons are given in table 1. PCR products were purified with a Qiagen PCR purification kit and genomic clones with a Qiagen Midiprep kit. PCR-generated templates were sequenced from both ends on an ABI 3100 capillary sequencer with ABI Big Dye chemistry or manually with a Thermo Sequenase radiolabeled terminator cycle-sequencing kit (USB). Alternatively, cDNA was reverse-transcribed (Omniscript RT kit, Qiagen) from RNA of Epstein-Barr virus (EBV)–transformed patient lymphoblasts and used for PCR amplification with exonic primers (Chan and Cole 1991). The products were sequenced and searched for heterozygous sequence variations or splicing variants. PCR-amplified

Table 1

Primers Used to Amplify ANK Exons from Genomic DNA of Individuals Affected with CMD

EXON	PRIMER (5′→3′)	
	Forward	Reverse
1	GATGGACTTGAGCTTGCGGATC	AGAGGGACTCGGAGCAGGTGAC
2	TGCAGTGGTCAGGTATCTCCTTC	GTCTTAAGCTAGGAGCACAAGCG
3	AACCCAGAGCATTCATTGGCTG	GAATGTACTTCCTGCCATTAAGC
4	CTGGGCTGCTAAGGCTTTGAG	CGGTGCTGGCAAAACCAGGTC
5	GTCAAGATCTTTGCTCAGAGGTC	CTTGGCCTCTGGGTATGACATC
6	GCAGCTTGCCAGCTGTCTCGG	GGCTTCCTAGTGTGACTGTCATG
7	CTGTCCTCAGTGGCTGCACC	AGGGAAGCAGGACTGAGAAGC
8	CCGCCTGGCAAACTGTCACTTG	GAAGAGATTGCTAATTAATCCAGCATC
9	CATGCCCACCACCCAGTCAG	GCATCTTTCTAAGCCACAGTG
10	CAGCGGCTCAACAGCAAGGC	GGATCCCAAGAGCCTCCACCTG
11	GAAGCCAGCAGATGGAGAACG	CACCCTAAGCCACGAGACTGG
12	GCTAAGATGCAAAAGAGGTGACG	CAACAGTAAAGACCATTCACTAGG
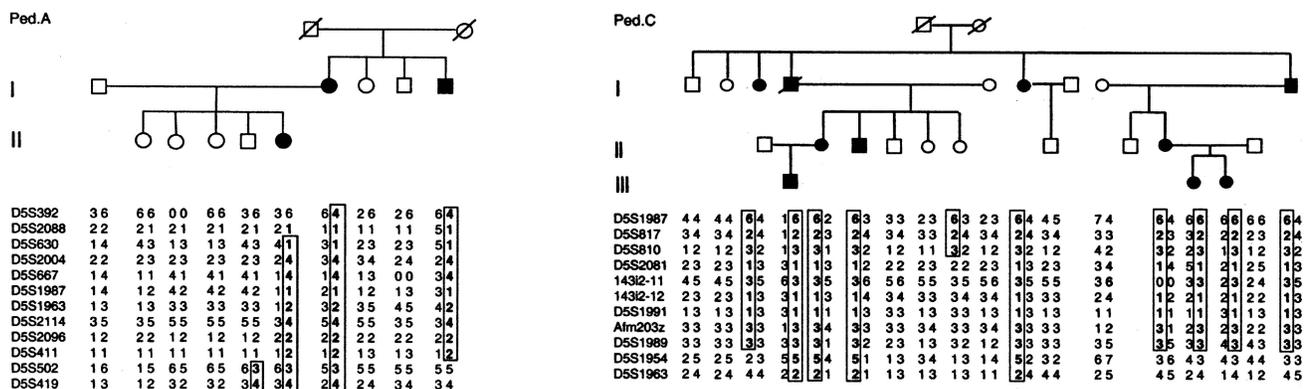
Figure 2 Pedigree of family A shows haplotypes for selected markers in the CMD locus on chromosome 5p, defining an initial 30-cM disease-gene interval. Recombinations in family C reduced the size of the locus to 5 cM, with breakpoints between markers D5S810 (telomeric) and D5S1954 (centromeric). The most likely haplotypes for the linked allele are boxed.

products containing putative mutations were cloned into PCRII-TOPO TA cloning vectors (Invitrogen) for clonal selection, and several clones for each mutation were sequenced. Variations in patient and wild-type sequences were examined, using BLAST. Electropherograms were examined visually for heterozygosities.
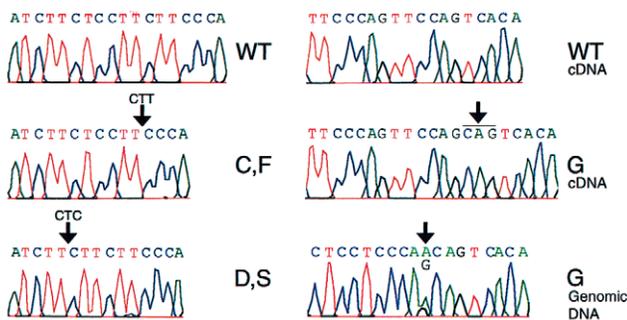
ANK Expression

cDNA was prepared with an Omniscript RT kit (Qiagen), and fragments were amplified using Hotstart *Taq* polymerase (Qiagen). A 716-nt fragment of *ANK* was amplified with primers ANK820up (5′-gtggcgattttgacagccacatac-3′) and ANK12dw (5′-gatgccgaagtgtcatcctga-

Figure 3 Electropherograms of partial sequences of *ANK* showing deletions and an insertion in families with CMD. Sequence variations are indicated by arrows (↓). Capital letters next to electropherograms indicate wild-type sequence (WT) and families and sporadic cases for which the respective mutation was tested. Electropherograms for families C, F and D, S show the sequence of the disease allele after clonal selection of PCR fragments from ANK exon 9 amplified from genomic DNA. The electropherograms for family G show wild-type (WT) and mutant allele carrying the insertion from cDNA after clonal selection, and the heterozygous A→G transition in intron 9 from genomic DNA.

ctg-3′) in 40 cycles (94°C for 30 s, 58°C for 30 s, and 72°C for 1 min) after a 15-min initial denaturation at 95°C. A 553-nt GAPDH fragment was amplified with primers G3PDH-F (5′-gaccacagtccatgccatcact-3′) and G3PDH-R (5′-tccaccaccctgttgctgtag-3′) in 30 cycles (94°C for 30 s, 58°C for 30 s, and 72°C for 2 min) after a 15-min initial denaturation at 95°C.
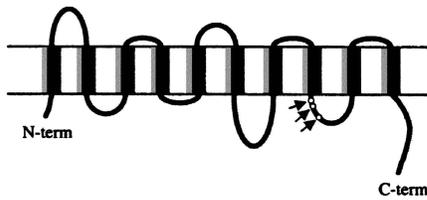
Results

For this study, we recruited five families (families A, B, C, G, and F) with AD inheritance of CMD and five families (families D, E, X1, X2, and S) with sporadic cases of CMD. Families A, B, C, G, and F include a total of 64 participating members, 37 of them affected with CMD; 23 (62%) of these affected individuals are female and 14 (38%) are male. The female:male ratio for all affected members of the families is similar, namely 59:41. The transmission of the CMD phenotype is complete in all families, but the expressivity varies. Some individuals are severely affected, whereas others show only mild expression of the disease. There is no evidence for anticipation, although there are some children who needed surgical intervention, early in childhood, to decompress facial nerve canals.

In the course of a genomewide screen, we initially identified a 30-cM locus between markers D5S2088 and D5S502 for family A (fig. 2) (Dib et al. 1996) (National Center for Biotechnology Information [NCBI] Map Viewer). Family B (data not shown) colocalized and showed no recombination within this region. This locus is confirmed by independent data from other groups, who mapped the AD CMD locus to a 19-cM region (Nurnberg et al. 1997) and an 11-cM region (J. Gardner, P. Beighton, H. Hamersma, S. Sellars, and R. Ramesar, unpublished data) within this interval. With family C

Figure 4 Locations of ANK mutations in patients with CMD (model of ANK according to Ho et al. 2000). The mutations cluster in a cytoplasmic domain between two putative transmembrane domains (mutations are indicated by arrows [→]).

(fig. 2), we were then able to restrict the locus to an interval between D5S810 and D5S1954, which corresponds to a physical size of 2–3 Mb (Church et al. 1997; R. Shiang, unpublished data) or to ~5 cM, according to the NCBI Map Viewer. To increase the resolution of the interval, we identified several new microsatellite repeats on BAC and PAC clones. Sequencing of the genomic clones with degenerate N(GT)$_8$ primers (Hawkins et al. 1994) resulted in a number of new dinucleotide-repeat markers. New repeat markers relevant for fine mapping were 143i2-11 (143i2-11UP: 5′-GAGGCAGGAGAATGCCTGAGCC-3′ and 143i2-11DW: 5′-CCACCGCACACTACTGACCAAAAC-3′), 143i2-12 (143i2-12UP: 5′-GCCAGGCATGGTAGTG-TGCGTC-3′ and 143i2-12DW: 5′-GCATGTGTCTCC-CATTGGCGTT-3′). Tight linkage for family C was found between D5S2081 (LOD score 3.4) and 143i2-12 (LOD score 3.9).

The CMD interval contains only two fully described genes but numerous expressed sequence tags. *TRIO* (Debant et al. 1996), which is implicated in actin polymerization, was considered an obvious candidate gene because of its possible function during actin reorganization in osteoclasts, but it was excluded by direct sequencing of genomic and cDNA fragments. Another candidate, *ANK*, was recently assigned to chromosome 5p (Ho et al. 2000). We screened a panel of individuals affected with CMD for nucleic acid changes in *ANK* by direct sequencing of genomic *ANK* PCR products (forward and reverse). We found two in-frame deletions for families C, F, D, and S in exon 9, and we detected one in-frame insertion in exon 10 for family G (fig. 3). All deletions and the insertion found are located within seven amino acids in the cytosolic domain between transmembrane domains 8 and 9 (fig. 4). The deletions of three nucleotides in exon 9 (TCT$_{1127–1129}$ in AD families C and F and CTC$_{1122–1124}$ in the sporadic cases D and S) result in the deletion of Phe$_{376}$ and Ser$_{375}$, respectively (table 2). By direct sequencing of cDNA products from affected members of the AD family G, we detected the insertion of an extra alanine between Pro$_{380}$ and Val$_{381}$ (fig. 5). Direct sequencing of a genomic PCR

fragment of exon 10 revealed a heterozygous nucleotide change (a→g) at position −4 at the splice-acceptor site of intron 9. The a→g transition produces a novel splice-acceptor site, which leads to the retention of three bases (cag) in the cDNA sequence. Exon 9 ends with a split codon (G), which contributes to the codon (GCA) for alanine. Testing on the genomic level showed that the mutation cosegregates in family G. We also tested cDNA from four affected and four unaffected members of family G and found cosegregation of the phenotype at the cDNA level. None of the sequence variants have been found in a panel of 80 unaffected control individuals.

By reverse transcriptase (RT)–PCR, we show that the mRNA for *ANK* is expressed in normal osteoblasts (fig. 6) from mandibular bone and from iliac bone, which have been kept in primary cell culture for three passages. The mRNA could not be detected in cultured osteoclastic cells from human osteoclastoma, which had been highly purified with the 23c6 anti–vitronectin-receptor antibody (a gift from G. D. Roodman).

Discussion

In this study, we describe the identification of mutations in *ANK*, which can cause CMD in families with AD CMD and in sporadic cases. The *ANK* gene encodes a 492–amino acid multipass transmembrane protein with 10 potential transmembrane domains.

All mutations described here are located in a cytosolic domain 4–10 amino acid residues C-terminal of the eighth transmembrane domain and 23–29 amino acid residues N-terminal of the ninth transmembrane domain. The mutations consist of two different in-frame single–amino acid deletions and one in-frame insertion of a single amino acid. The deletions were detected by direct sequencing of genomic fragments (families C, F, D, and S) as well as by sequencing cDNA from EBV-transformed lymphoblasts (families C, D, and S). The
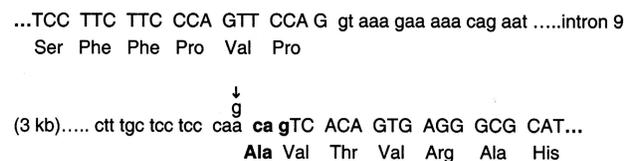
Figure 5 Exon-intron boundaries of *ANK* exons 9 and 10. Capital letters indicate exon sequences; lowercase letters indicate intron sequences. Three nucleotides on the splice-acceptor site of intron 9, which are retained in the cDNA sequence of family G, are marked in boldface type. Exon 9 ends with a split codon, which contributes to the codon (GCA) for the extra alanine. The new splice-acceptor site in the disease allele is created by the heterozygous point mutation (a→g) in position −4 of the splice-donor site of intron 9 (marked by an arrow (↓).

Table 2

Mutations in *ANK* That Cause CMD

Mutation	Change	Family or Families
Deletion:		
$TCT_{1127-1129}$	ΔPhe_{376}	C and F
$CTC_{1122-1124}$	ΔSer_{375}	D and S
Insertion:		
$CAG_{1139-1141}$	Ala_{380}	G

insertion of a single alanine was detected in cDNA of family G, but the mutation itself is a point mutation (a→g transition) in the splice-acceptor site of intron 9. This leads to the creation of a cryptic splice site and to the retention of three nucleotides in exon 10. We are confident that the described sequence variants are mutations (1) because of the accumulation of three different variants in the same domain of *ANK* in individuals with CMD, (2) because all the variants cosegregated with the phenotype in the respective families, and (3) because these variants were not found in parents or siblings of the individuals representing sporadic cases. None of the deletions were found in a panel of 80 unaffected control individuals. Interestingly, no mutations have been found either in families A and B or in the sporadic cases X1, X2, and E, despite thorough sequencing of genomic DNA and sequencing of cDNA from two affected individuals in pedigree A. Since families A and B were initially used to map the CMD locus in our laboratory, we think it is possible that CMD in these two families is caused by mutations in *cis*-acting regulatory elements, such as in the promoter or enhancer/silencer regions of *ANK*. In this case, compromised expression of *ANK* could result in haploinsufficiency. We cannot, at this point, exclude positional effects (Kleinjan and van Heyningen 1998), which can be caused by chromosomal rearrangement outside the transcription and promoter regions. Finally, it is possible that there is genetic heterogeneity, especially for the sporadic cases X1, X2, and E. A distinct locus for AR CMD (Iughetti et al. 2000) has already been described on chromosome 6q21-22.

Expression of mouse *ank* has been found in articular cartilage and in many nonskeletal tissues (Ho et al. 2000). We showed by RT-PCR that the mRNA is expressed in osteoblasts from primary cell culture but was not detected in cultured osteoclastic cells from human osteoclastoma, which had been highly purified with the 23c6 anti–vitronectin-receptor antibody (fig. 6). ANK is likely to be a multipass transmembrane protein, and functional studies suggest that ANK is involved in transport or cotransport of intracellular pyrophosphate (PPi) into extracellular matrix (Ho et al. 2000).

A nonsense mutation in mouse *ank* results in a pre-mature stop codon. In homozygous mice, the expression of the ank protein is ablated or at least reduced below detectable levels (Ho et al. 2000). Overexpression of the murine *ank* mutation in cultured cells results in increased intracellular and decreased extracellular PPi concentration. Skeletal pyrophosphate levels are critical for regulation of mineralization in bone. Increased extracellular PPi concentrations, such as in hypophosphatasia (tissue-nonspecific alkaline phosphatase [MIM 146300]) (Caswell et al. 1991), have a negative effect on bone mineralization; thus, decreased levels of extracellular PPi in bone may result in increased bone density. Therefore, it is likely that mutations in *ANK* of patients with CMD lead to decreased PPi levels in bone extracellular matrix, which in turn cause increased density and progressive thickening of cranial bones. It may well be the change in mineral content that prevents osteoclasts from remodeling cranial bone at a normal rate.

Homozygous *ank/ank* mutant mice develop progressive generalized ankylosis of joints (Sweet and Green 1981), whereas heterozygous mice show no detectable phenotype. Although the murine *ank* mutation results in a loss of function, the mutations found in CMD patients are likely to have a dominant negative effect on the function of ANK. However, if future research shows that mutations in *cis*-acting regulatory elements can also lead to CMD in humans, reduced ANK expression would also have to be considered as a cause for CMD. It is possible that there is a dose effect of ANK expression in humans, resulting in CMD, although heterozygous *ank* mice do not have a detectable phenotype.

The radiolucent, flared metaphyses in CMD patients are likely to be the result of a remodeling defect. Hypertrophic cartilage in normal epiphyseal growth plates is calcified before it is degraded and primary bone is formed. Decreased levels of PPi in hypertrophic cartilage of patients with CMD may affect calcification, normal cartilage degradation, and osteoid deposition, which in the end affects proper trabeculation of the metaphyses.

All the mutations found to date localize to a putative cytosolic domain of *ANK* and are either an insertion or a deletion of one amino acid. Therefore, it is conceivable that this domain is critically involved in complex for-
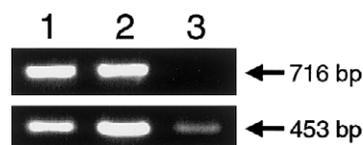
Figure 6 *Upper panel,* Expression of *ANK* by RT-PCR from cultured osteoblasts from mandibular (*lane 1*) and iliac (*lane 2*) bone, and from osteoclasts from osteoclastoma (*lane 3*). *Lower panel,* GAPDH fragments were amplified as internal controls.

mation with another protein or in interaction with pyrophosphate or another small molecule involved in pyrophosphate transport, although no similarity to known domains has been found so far. CMD mutations provide a good genetic model to study the regulation of bone mineralization by inorganic phosphate and the precise role of *ANK* in PPi transport mechanisms. These studies may, in the future, benefit not only patients with CMD but also patients with deficiencies in skeletal mineralization.

Acknowledgments

Electronic-Database Information

Celera, http://www.celera.com/

FACES: The National Craniofacial Association, http://www.faces-cranio.org/

GenBank, http://www.ncbi.nlm.nih.gov/Genbank/index.html

Genome Database, http://gdbwww.gdb.org/

Lawrence Berkeley National Laboratory Sequence Archive, http://www-hgc.lbl.gov/seq/

NCBI Map Viewer, http://www.ncbi.nlm.nih.gov/cgi−bin/Entrez/hum_srch?chr=hum_chr.inf

Online Mendelian Inheritance in Man (OMIM), http://www.ncbi.nlm.nih.gov/Omim/ (for AD CMD [MIM 123000], AR CMD [MIM 218400]), Pyle disease [MIM 265900]), craniodiaphyseal dysplasia [MIM 218300], frontometaphyseal dysplasia [MIM 305620]), osteopathia striata with cranial sclerosis [MIM 166500], sclerosteosis [MIM 269500], and hypophosphatasia [MIM 146300]).

References

Balemans W, Ebeling M, Patel N, Van Hul E, Olson P, Dioszegi M, Lacza C, Wuyts W, Van Den Ende J, Willems P, Paes-Alves AF, Hill S, Bueno M, Ramos FJ, Tacconi P, Dikkers FG, Stratakis C, Lindpaintner K, Vickery B, Foernzler D, Van Hul W (2001) Increased bone density in sclerosteosis is due to the deficiency of a novel secreted protein (SOST). Hum Mol Genet 10:537–543

Brunkow ME, Gardner JC, Van Ness J, Paeper BW, Kovacevich BR, Proll S, Skonier JE, Zhao L, Sabo PJ, Fu YH, Alisch RS, Gillett L, Colbert T, Tacconi P, Galas D, Hamersma H, Beighton P, Mulligan JT (2001) Bone dysplasia sclerosteosis results from loss of the SOST gene product, a novel cystine knot-containing protein. Am J Hum Genet 68:577–589

Caswell AM, Whyte MP, Russell RG (1991) Hypophosphatasia and the extracellular metabolism of inorganic pyrophosphate: clinical and laboratory aspects. Crit Rev Clin Lab Sci 28:175–232

Chan D, Cole WG (1991) Low basal transcription of genes for tissue-specific collagens by fibroblasts and lymphoblastoid cells: application to the characterization of a glycine 997 to serine substitution in α 1(II) collagen chains of a patient with spondyloepiphyseal dysplasia. J Biol Chem 266:12487–12494

Church DM, Yang J, Bocian M, Shiang R, Wasmuth JJ (1997) A high-resolution physical and transcript map of the Cri du chat region of human chromosome 5p. Genome Res 7:787–801

Debant A, Serra-Pages C, Seipel K, O'Brien S, Tang M, Park SH, Streuli M (1996) The multidomain protein Trio binds the LAR transmembrane tyrosine phosphatase, contains a protein kinase domain, and has separate rac-specific and rho-specific guanine nucleotide exchange factor domains. Proc Natl Acad Sci USA 93:5466–5471

Dib C, Faure S, Fizames C, Samson D, Drouot N, Vignal A, Millasseau P, Marc S, Hazan J, Seboun E, Lathrop M, Gyapay G, Morissette J, Weissenbach J (1996) A comprehensive genetic map of the human genome based on 5,264 microsatellites [see comments]. Nature 380:152–154

Gorlin RJ, Spranger J, Koszalka MF (1969) Genetic craniotubular bone dysplasias and hyperostostes: a critical analysis. Birth Defects Orig Art Ser 5:79–95

Hawkins GA, Bishop M, Kappes S, Beattie CW (1994) Cycle sequencing of (CA)n microsatellites from cosmid inserts using degenerate primers. Biotechniques 16:418–420

Ho AM, Johnson MD, Kingsley DM (2000) Role of the mouse ank gene in control of tissue calcification and arthritis. Science 289:265–270

Iughetti P, Alonso LG, Wilcox W, Alonso N, Passos-Bueno MR (2000) Mapping of the autosomal recessive (AR) craniometaphyseal dysplasia locus to chromosome region 6q21-22 and confirmation of genetic heterogeneity for mild AR spondylocostal dysplasia. Am J Med Genet 95:482–491

Jackson WPU, Albright F, Drewery G, Hanelin J, Rubin ML (1954) Metaphyseal dysplasia, epiphyseal dysplasia, diaphyseal dysplasia and related conditions. Arch Intern Med 94:871–885

Kleinjan DJ, van Heyningen V (1998) Position effect in human genetic disease. Hum Mol Genet 7:1611–1618

Nurnberg P, Tinschert S, Mrug M, Hampe J, Muller CR, Fuhrmann E, Braun HS, Reis A (1997) The gene for autosomal dominant craniometaphyseal dysplasia maps to chromosome 5p and is distinct from the growth hormone–receptor gene. Am J Hum Genet 61:918–923

Sweet HO, Green MC (1981) Progressive ankylosis, a new skeletal mutation in the mouse. J Hered 72:87–93

Tiziani V, Reichenberger E, Buzzo CL, Niazi S, Fukai N, Stiller M, Peters H, Salzano FM, Raposo do Amaral CM, Olsen BR (1999) The gene for cherubism maps to chromosome 4p16. Am J Hum Genet 65:158–166